Supplementary Information

A calcium-dependent acyltransferase that produces *N*-acyl phosphatidylethanolamines

Yuji Ogura, William H. Parsons, Siddhesh S. Kamat, Benjamin F. Cravatt*

Department of Chemical Physiology and The Skaggs Institute for Chemical Biology, The Scripps Research Institute, 10550 N. Torrey Pines Rd., La Jolla, CA 92037

*To whom correspondence should be addressed: cravatt@scripps.edu

Supplementary Results

Table of Contents

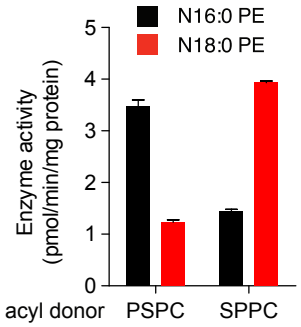

Supplementary Figure 1. Measure of *sn*-1 vs. *sn*-2 specificity for Ca-NAT activity in mouse brain membrane lysates. Lysates were incubated with *sn*-1, *sn*-2-dioleoyl-phosphatidylethanolamine (DOPE, 250 μM) and either *sn*-1-palmitoyl-*sn*-2-stearoyl phosphatidylcholine (PSPC) or *sn*-1-stearoyl-*sn*-2-palmitoyl phosphatidylcholine (SPPC) for 1 h at 37 °C with $CaCl_2$ (3 mM). The *N*-C16:0 DOPE and *N*-C18:0 DOPE products were measured. Data represent mean values ± s. d. for 3 biological replicates.

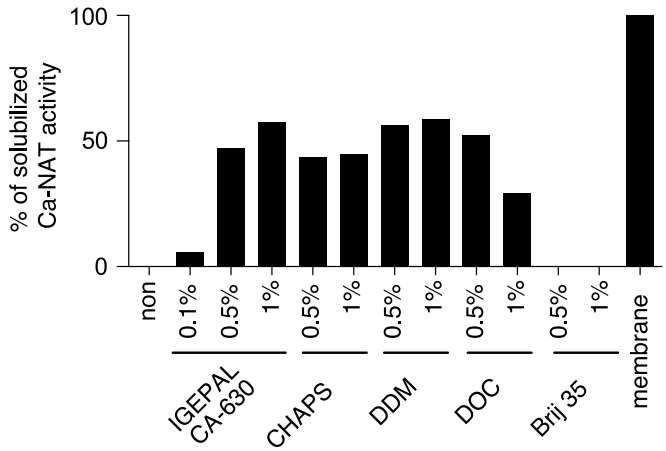

Supplementary Figure 2. Solubilizing Ca-NAT activity in the membrane fraction of mouse brain. Solubilized mouse brain membrane proteome was prepared with the indicated detergent, and its Ca-NAT activity was determined by incubating 40 µg of proteome with 250 µM DPPC, 250 µM DOPE, and 3 mM $CaCl_2$ for 1 h at 37 °C and measuring *N*-C16:0 DOPE production.

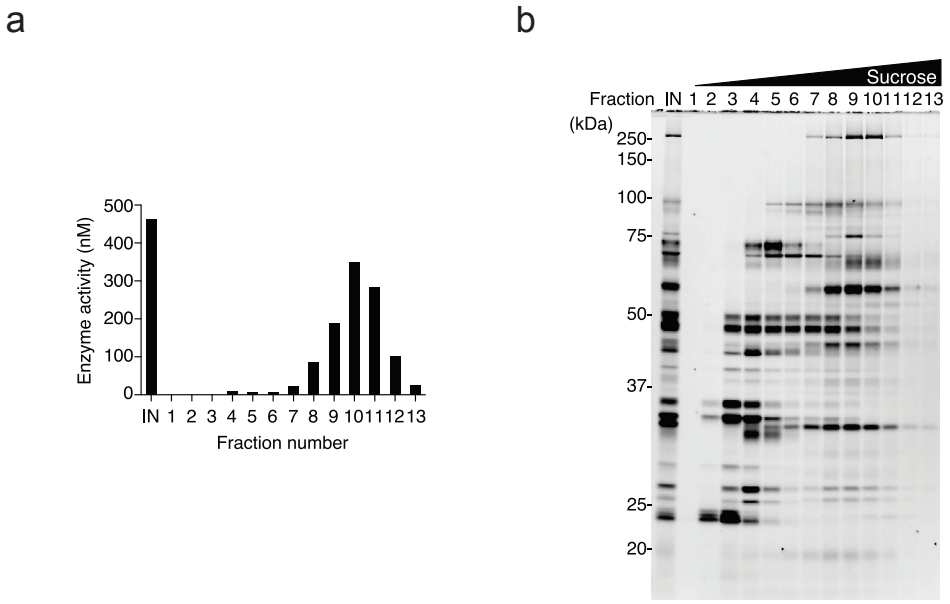

Supplementary Figure 3. Analysis of fractions from sucrose gradient centrifugation of mouse brain membrane lysates. (**a**) Ca-NAT activity of fractions obtained by sucrose gradient (5-40%) centrifugation of detergent-solubilized mouse brain membrane lysates. Fractions were incubated with *sn*-1, *sn*-2-dipalmitoyl-phosphatidylcholine (DPPC; 250 µM) and *sn*-1, *sn*-2-dioleoyl-phosphatidylethanolamine (DOPE, 250 µM) for 1 h at 37 °C with or without $CaCl_2$ (3 mM). The production of *N*-C16:0 DOPE was measured, and Ca-independent activities were subtracted in the calculations of Ca-dependent activity. Data represent activity measurements from one experiment representative of two biological replicates. (**b**) Gel-based ABPP of fractions, showing differential distribution of serine hydrolase activities detected by reactions with FP-rhodamine (1 µM, 30 min at 25 °C).

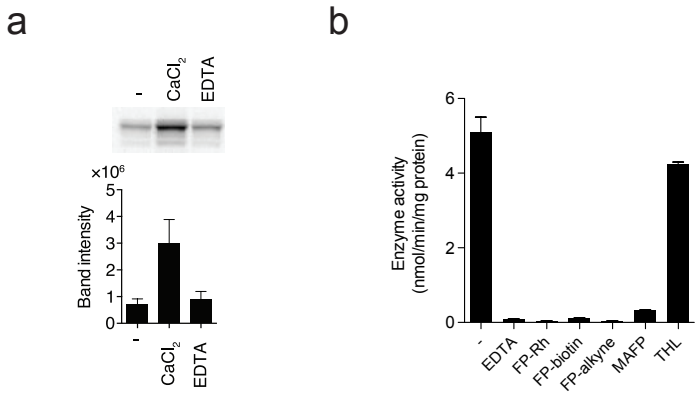

Supplementary Figure 4. Analysis of recombinant mouse PLA2G4E activity. **(a)** Gel-based ABPP analysis demonstrating calcium-enhanced FP-rhodamine labeling of recombinant mouse PLA2G4E in transfected, detergent-solubilized HEK293T cell lysates. The bands shown for PLA2G4E are from the full gel shown in **Figure 2a**. Band intensities were quantified using Image Lab software (BIO-RAD). Data represent mean values ± s. d. for 3 biological replicates. (**b**) Inhibitor sensitivity of Ca-NAT activity for recombinant PLA2G4E. PLA2G4E-transfected HEK293T lysate (+ 3 mM $CaCl_2$) was treated with or without EDTA (10 μM) or pre-treated with MAFP (3 μM), FP probes (1 μM), or THL (3 μM) for 30 min at 25 °C. *N*-C16:0 DOPE production was then measured in reactions with DPPC (40 μM) and DOPE (75 μM) for 30 min at 37 °C. Data represent mean values ± s. d. for 3 biological replicates.

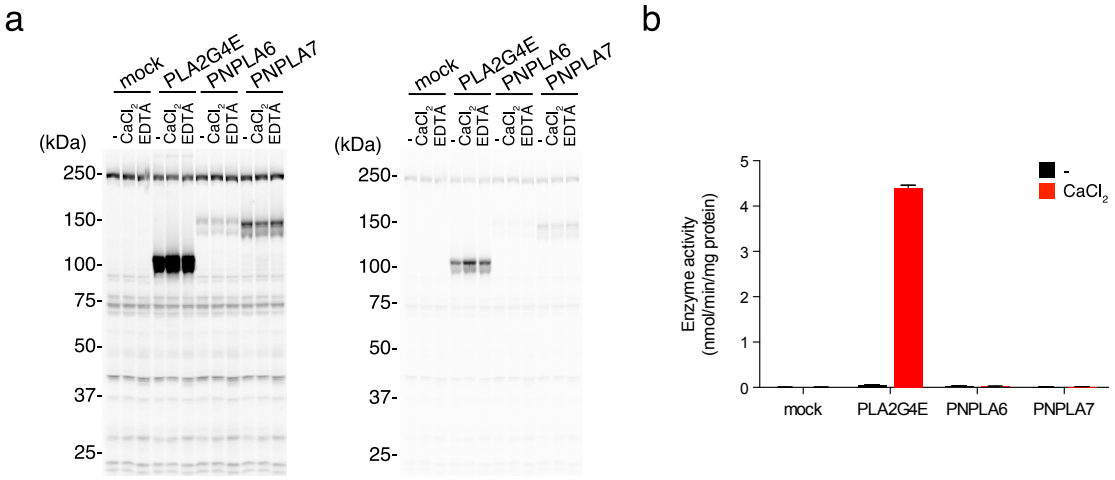

Supplementary Figure 5. Ca-NAT activity for recombinant PLA2G4E, PNPLA6, and PNPLA7. (**a**) ABPP gel (left: 60 sec exposure; right: 2 sec exposure) demonstrating overexpression of mouse PLA2G4E, mouse PNPLA6, and mouse PNPLA7 in HEK293T cells. Proteomes were incubated with 1 μM FP-Rh for 30 min at 25 °C in the presence or absence of 3 mM $CaCl_2$ or 10 mM EDTA. (**b**) Ca-NAT activity of transfected HEK293T lysates as measured by *N*-C16:0 DOPE production. 2 μg of proteome was incubated with 40 μM DPPC and 75 μM DOPE for 30 min at 37 °C in the presence or absence of 3 mM $CaCl_2$. Data represent mean values ± s. d. for 3 biological replicates.

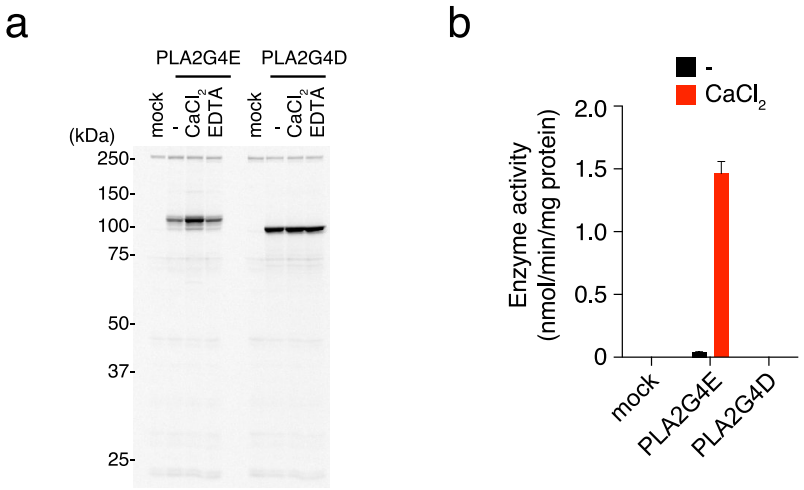

Supplementary Figure 6. Ca-NAT activity for recombinant PLA2G4E versus PLA2G4D. (**a**) ABPP gel demonstrating overexpression of mouse PLA2G4E and mouse PLA2G4D in HEK293T cells. Proteomes were incubated with 1 μM FP-Rh for 30 min at 37 °C in the presence or absence of 3 mM $CaCl_2$ or 10 mM EDTA. (**b**) Ca-NAT activity of transfected HEK293T lysates as measured by *N*-C16:0 DOPE production. 2 μg of proteome was incubated with 40 μM DPPC and 75 μM DOPE for 30 min at 37 °C in the presence or absence of 3 mM $CaCl_2$. Data represent mean values ± s. d. for 3 biological replicates.

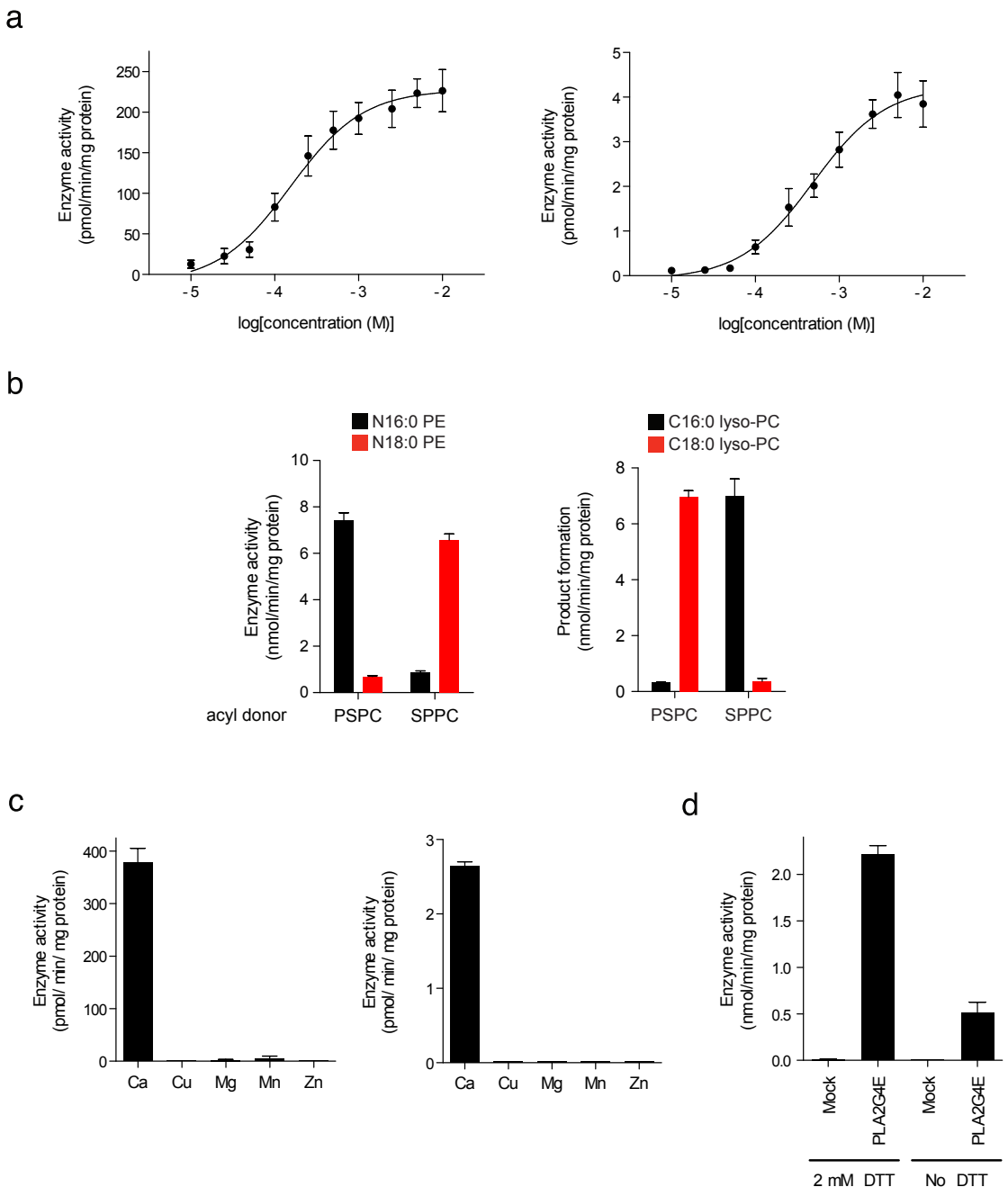

Supplementary Figure 7. Calcium-dependence and acyl chain selectivity of PLA2G4E. (**a**) Calcium concentration-response curves for the detergent-solubilized membrane fractions of PLA2G4E-transfected HEK293T cells (left) and mouse brain (right). 40 µg of proteome was incubated with 250 µM DPPC and 250 µM DOPE for 1 h at 37 °C in the presence of the indicated concentration of $CaCl_2$. Enzyme activity was determined by measuring the production of *N*-C16:0 DOPE. An EC_{50} of 0.16 mM $CaCl_2$ (95% confidence intervals of 0.08-0.29 mM) was determined for recombinant PLA2G4E and an EC_{50} of 0.49 mM $CaCl_2$ (95% confidence intervals of 0.28-0.85 mM) for mouse brain. (**b**) Production of *N*-

C16:0 DOPE and *N*-C18:0 DOPE (left) and C16:0 lyso-PC and C18:0 lyso-PC (right) by PLA2G4E. 2 μg of proteome from PLA2G4E-transfected HEK293T cells was incubated with 75 μM DOPE and 40 μM of either *sn*-1-palmitoyl-*sn*-2-stearoyl phosphatidylcholine (PSPC) or *sn*-1-stearoyl-*sn*-2-palmitoyl phosphatidylcholine (SPPC) for 30 min at 37 °C in the presence of 3 mM $CaCl_2$. (**c**) Production of *N*-C16:0 DOPE by detergent-solubilized membrane fractions of PLA2G4E-transfected HEK293T cells (left) and mouse brain (right) in the presence of divalent cations. 40 μg of proteome was incubated with 250 μM DPPC and 250 μM DOPE for 1 h at 37 °C in the presence of 10 mM of the chloride salt of the indicated cation. (**d**) Effect of DTT on the Ca-NAT activity of PLA2G4E. 2 μg of proteome from PLA2G4E-transfected HEK293T cells was incubated with 40 μM of DPPC and 75 μM DOPE for 30 min at 37 °C in the presence of 3 mM $CaCl_2$ with or without the addition of 2 mM DTT. For assays with recombinant PLA2G4E in **a** and **c**, 4 μg of proteome from PLA2G4E-transfected HEK293T cells was combined with 36 μg of proteome from mock-transfected HEK293T cells. Data for **a**-**d** represent mean values ± s. d. for 3 biological replicates.

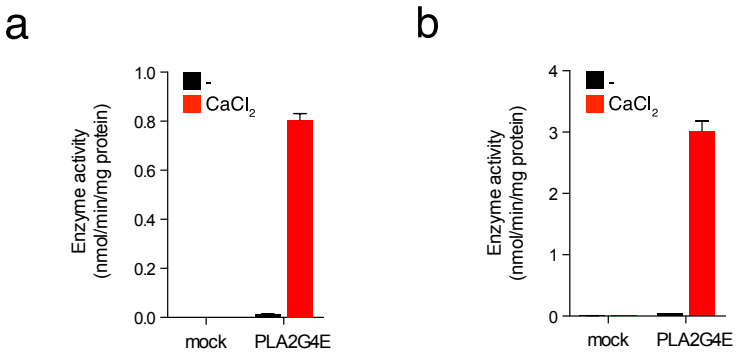

Supplementary Figure 8. Recombinant PLA2G4E generates the anandamide precursor *N*-C20:4 NAPE and can use phosphatidylethanolamine (PE) as an acyl donor. (**a**) Production of *N*-C20:4 DOPE by PLA2G4E. 2 µg of lysate was incubated with 40 µM *sn*-1, *sn*-2-diarachidonoyl-phosphatidylcholine and 75 µM DOPE for 30 min at 37 °C in the presence or absence of 3 mM $CaCl_2$. (**b**) Production of *N*-C18:1 DOPE from dioleoyl PE (DOPE) by PLA2G4E. 2 µg of lysate was incubated with 75 µM DOPE alone for 30 min at 37 °C in the presence or absence of 3 mM $CaCl_2$. Data for **a** and **b** represent mean values ± s. d. for 3 biological replicates.

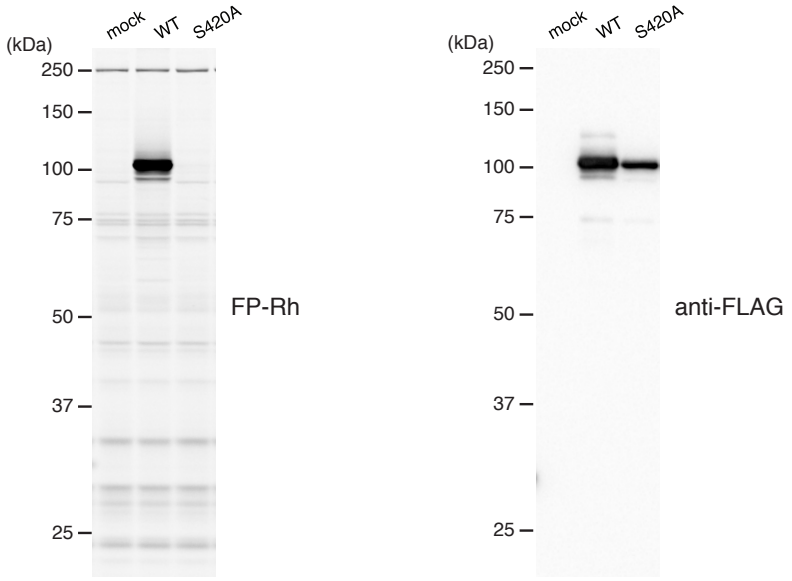

Supplementary Figure 9. Gel-based ABPP and Western blot analyses of transfected HEK293T proteomes (0.3 mg mL^{-1}) showing selective labeling by FP-rhodamine (1 μM) of WT-PLA2G4E but not the S420A mutant.

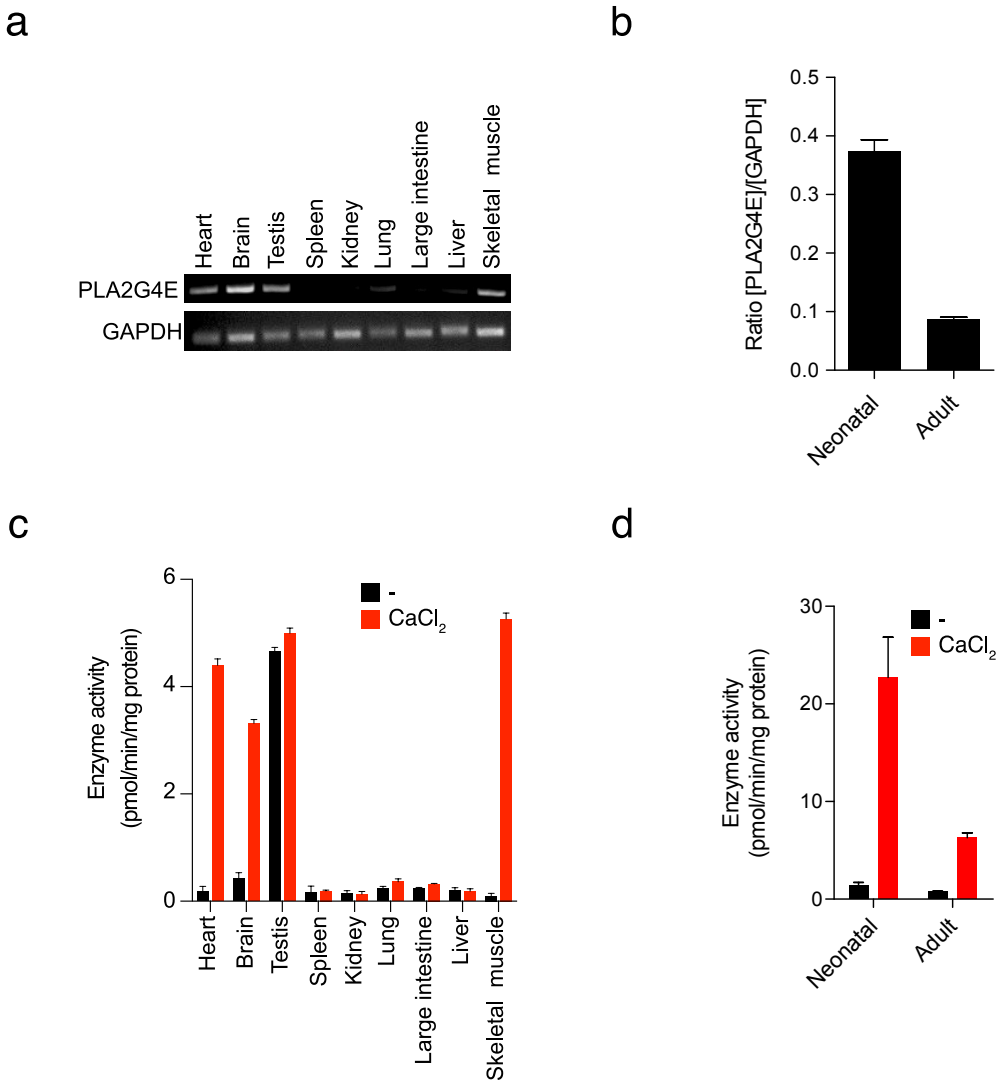

Supplementary Figure 10. Distribution of PLA2G4E expression and Ca-NAT activity in mouse tissues. (**a**) RT-PCR analysis of PLA2G4E expression in nine different mouse tissues. GAPDH was used as a standard. (**b**) RT-PCR analysis of PLA2G4E expression in neonatal (day 1 post-natal) and adult male (10-week-old) mouse brain. Data represent mean values ± s. d. for 4 biological replicates. GAPDH was used as a standard. (**c**) Ca-NAT activity of mouse tissue proteomes as measured by *N*-C16:0 DOPE production. 40 μg of proteome was incubated with 250 μM DPPC and 250 μM DOPE for 1 h at 37 °C in the presence and absence of 3 mM $CaCl_2$. Data represent mean values ± s. d. for 3 biological replicates. (**d**) Ca-NAT activity of brain proteomes from neonatal and adult mice as measured by *N*-C16:0 DOPE production. 40 μg of proteome was incubated with 250 μM DPPC and 250 μM DOPE for 1 h at 37 °C in the presence and absence of 3 mM $CaCl_2$. Data represent mean values ± s. d. for 3 biological replicates.

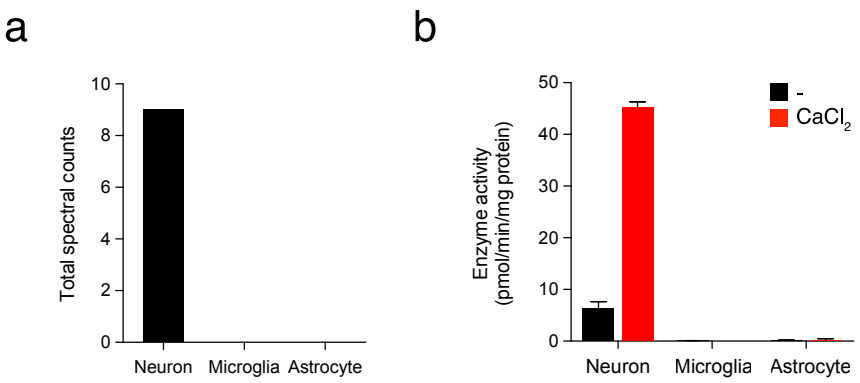

Supplementary Figure 11. Distribution of PLA2G4E expression and Ca-NAT activity in mouse brain. (**a**) Spectral counts for PLA2G4E in neurons, microglia, and astrocytes from previous ABPP-MudPIT experiments performed using the FP-biotin probe. Data obtained from experiments described in Ref. 1. (**b**) Ca-NAT activity of lysates prepared from neurons, microglia, and astrocytes as measured by *N*-C16:0 DOPE production. 2.5 μg of proteome was incubated with 40 μM DPPC and 75 μM DOPE for 1 h at 37 °C in the presence or absence of 3 mM $CaCl_2$ or 10 mM EDTA. Data represent mean values ± s. d. for 3 biological replicates.

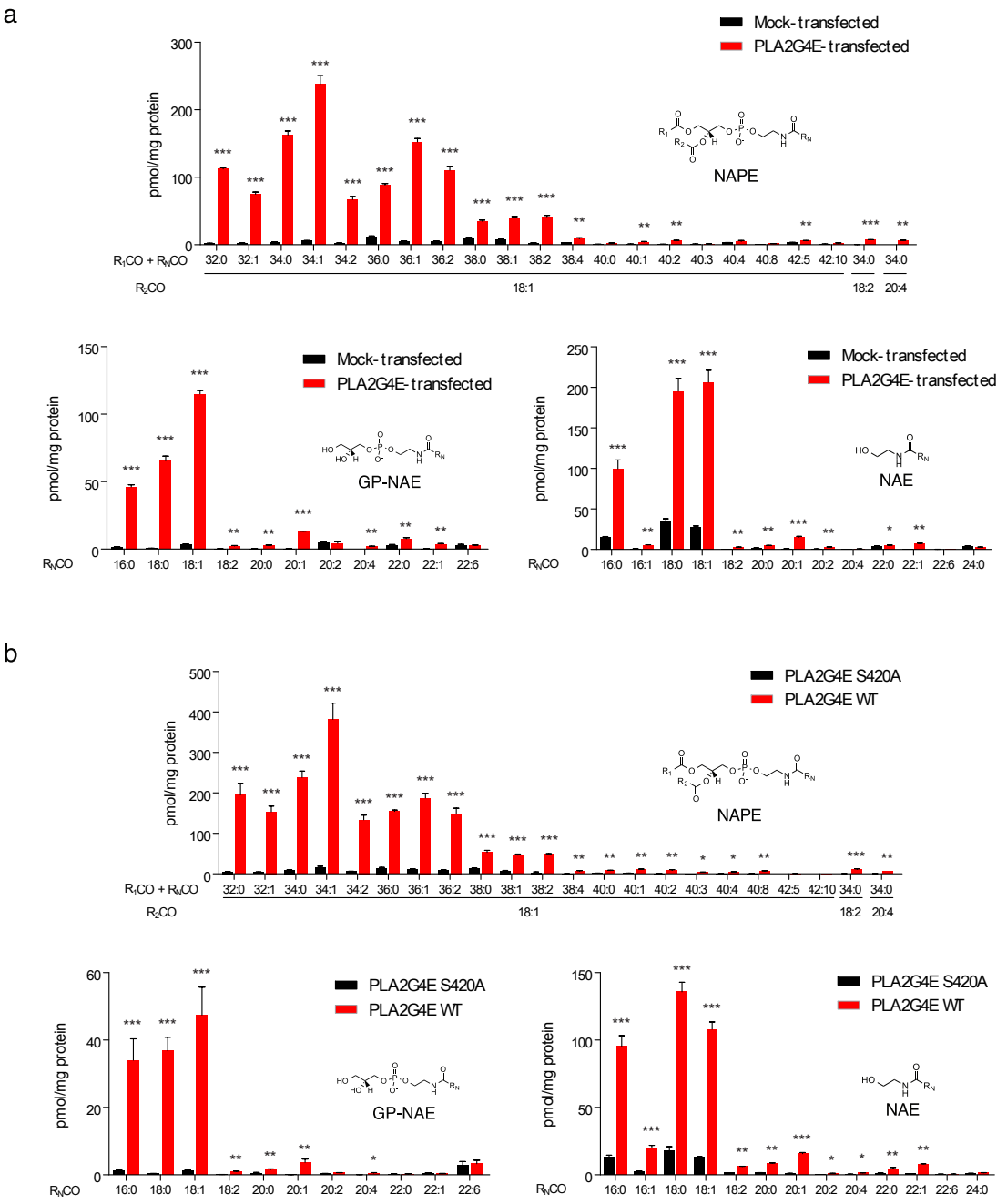

Supplementary Figure 12. Production of NAPEs, GP-NAEs, and NAEs in transfected HEK293T cells. (**a**) Comparison of lipids from cells transfected with either WT PLA2G4E or empty vector (mock). 48 h after transfection, lipids were extracted and analyzed by LC-MS/MS. (**b**) Comparison of lipids from cells transfected with either WT PLA2G4E or the S420A mutant. Data for **a** and **b** represent mean values ± s. d. for 3 biological replicates. *, $p < 0.05$, **, $p < 0.01$, *** $p < 0.001$ by two-sided Student's *t*-test for WT PLA2G4E-transfected vs either mock- or S420A PLA2G4E-transfected cells.

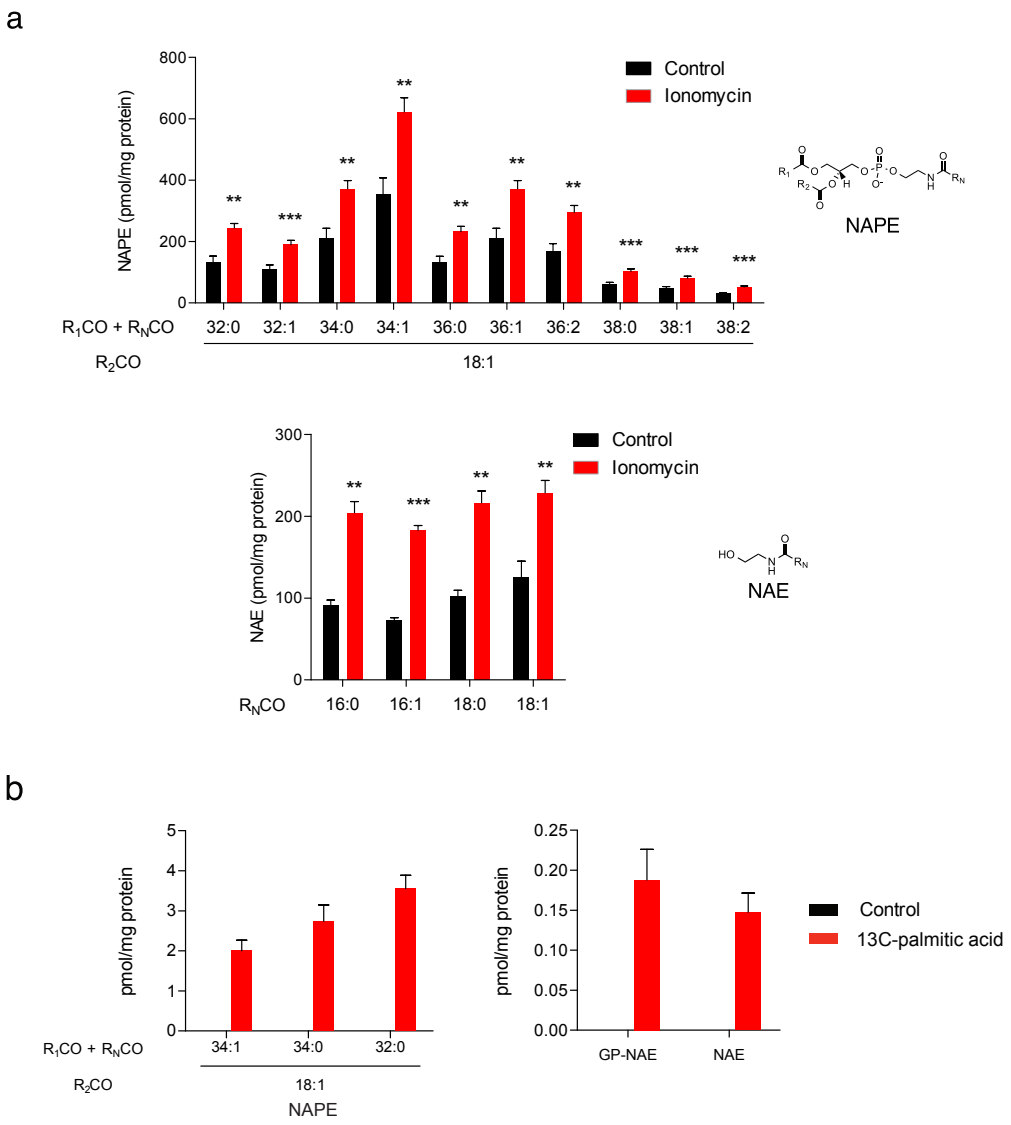

Supplementary Figure 13. Production of NAPEs, GP-NAEs, and NAEs in PLA2G4E-transfected HEK293T cells in response to ionomycin treatment or ^{13}C-palmitic acid feeding. (**a**) Comparison of lipids from PLA2G4E-transfected cells incubated in the presence or absence of 2 μM ionomycin for 4 h. Following the incubation, lipids were extracted and analyzed by LC-MS/MS. (**b**) Comparison of ^{13}C-labeled lipids from PLA2G4E-transfected cells incubated in the presence or absence of $^{13}C_{16}$-palmitic acid (250 μM) for 4 h. Following the incubation, lipids were extracted and analyzed by LC-MS/MS. Data for **a** and **b** represent mean values ± s. d. for 3 biological replicates. *, $p < 0.05$, **, $p < 0.01$, *** $p < 0.001$ by two-sided Student's *t*-test for ionomycin-treated vs control (DMSO)-treated PLA2G4E-transfected cells.

Supplementary Table 1. Complete ABPP-MudPIT data set. See attached Excel file.

Tab 1 ('Serine hydrolases'). Spectral counts for serine hydrolases detected in the ABPP-MudPIT analysis of fractions 2-13 from separation of mouse brain membrane proteome over sucrose gradient. Calculated Pearson correlation coefficients for each serine hydrolase are presented in the far right column.

Tab 2 ('All proteins'). Spectral counts for all proteins detected in the ABPP-MudPIT analysis of fractions 2-13 from separation of mouse brain membrane proteome over sucrose gradient. Calculated Pearson correlation coefficients for each protein are presented in the far right column.

Supplementary References

1 Viader, A.; Ogasawara, D.; Joslyn, C. M.; Sanchez-Alavez, M.; Mori, S.; Nguyen, W.; Conti, B.; Cravatt, B. F. A chemical proteomic atlas of brain serine hydrolases identifies cell type-specific pathways regulating neuroinflammation. *eLife* doi: 10.7554/eLife.12345 (2016).